Submitted to Physics of Fluids

LBL-3270
Preprint C.

PARAMETRIC INSTABILITIES IN PLASMA WITH SINUSOIDAL DENSITY MODULATION

Dwight R. Nicholson

June 20, 1975

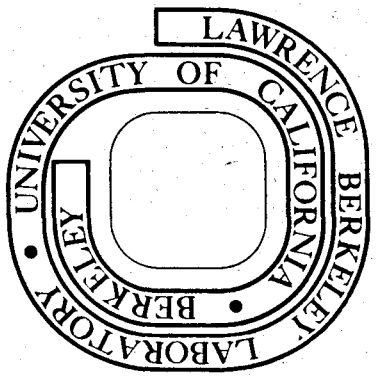

Prepared for the U. S. Energy Research and Development Administration under Contract W-7405-ENG-48

DISCLAIMER

PARAMETRIC INSTABILITIES IN PLASMA WITH SINUSOIDAL DENSITY MODULATION*

Dwight R. Nicholson†

Lawrence Berkeley Laboratory
University of California
Berkeley, California 94720

June 20, 1975

ABSTRACT

Parametric instabilities in the presence of sinusoidal plasma density modulation are considered analytically and by numerical integration of the coupled mode equations. The density modulation tends to reduce temporal and spatial growth rates. If there is a linear density gradient in addition to the density modulation, the usual convective saturation exists for small modulation; however, above a certain threshold modulation, the convective saturation is replaced by absolute growth. This result is in qualitative agreement with earlier work[1] on plasma with linear density gradient plus turbulence.

I. INTRODUCTION

Parametric instabilities in spatially inhomogeneous plasma have been extensively studied; see Ref. 1 and citations therein. Much of the work has dealt with monotonic inhomogeneities, while a few papers[1-4] have treated the important problem of nonmonotonic, turbulent-like inhomogeneities. Many of the effects of nonmonotonic inhomogeneity depend on amplitude and scale length, rather than detailed spatial profile. We therefore consider here the tractable problem of a

sinusoidal density modulation, in the presence and in the absence of a linear density gradient.

Let us briefly review related work. The problem of three-wave interactions in the presence of random stationary background fluctuations was first considered by Tamoikin and Fainshtein.[4] The coupled mode equations for all three waves were treated, assuming small relative density fluctuations, and it was found that the relaxation oscillations are suppressed by the turbulence. Wilhelmsson[5] also treated all three waves, studying the related problem of the temporal evolution of small initial phase uncertainties.

The closely related problem where one wave, the pump, has fixed amplitude but random phase variations (finite bandwidth), has been treated by many authors, including Thomson,[6] Pellat, Pesme, and Laval,[7] and Rosenbluth and Williams[8] (see Ref. 1 for earlier references). An important effect is usually found when the bandwidth is of the same order as the zero-bandwidth instability growth rate.

When all inhomogeneities (assumed one-dimensional) have a much longer scale length than the wavelengths of the three coupled modes, and when the amplitude of one wave (the pump) can be considered essentially constant in space and time, the following equations apply for the slowly varying amplitudes $a_1(x,t)$, $a_2(x,t)$ of the other two coupled modes, the decay waves:[9-11]

$$(\partial_t + \nu_1 + V_1\partial_x)\, a_1(x,t) = \gamma_0\, a_2(x,t) \exp\left[i \int_0^x \kappa(x')dx' \right] ,$$

Equation (1) continued next page

Equation (1) continued

$$(\partial_t + \nu_2 + V_2\partial_x)\, a_2(x,t) = \gamma_0\, a_1(x,t) \exp\left[-i\int_0^x \kappa(x')dx'\right]. \tag{1}$$

Here ν_1,ν_2 are the linear damping rates; V_1,V_2 are the x-components of the group velocities, having either sign; γ_0 is a positive constant, proportional to the amplitude of the pump wave, and is the temporal growth rate of the instability in the absence of damping, plasma inhomogeneity, and spatial variation of the amplitudes; while $\kappa(x)$ is the wave number mismatch between the three waves, whose frequencies match exactly; the origin $x = 0$ is chosen as a point where the spatially dependent wavenumbers match exactly; i.e., $\kappa(x = 0) = 0$.

These equations are characterized by the basic length $L_0 \equiv |V_1V_2|^{\frac{1}{2}}/\gamma_0$, which is the steady state, homogeneous medium spatial growth rate when $V_1V_2 > 0$, $\nu_1 = \nu_2 = 0$. Kaw et al.[2] have considered the case $V_1V_2 > 0$, assuming a steady state in time, with the mismatch $\kappa(x)$ caused by spatial plasma turbulence and characterized by rms amplitude Δ and correlation length $L_T \ll L_0$, and with damping neglected. In the absence of a linear density gradient, assuming $\Delta^2 L_T L_0 \gg 1 \gg L_T/L_0$, they found that the growth length (L_0 in the absence of turbulence) was increased by the large factor $\Delta^2 L_T L_0$. In the presence of a linear density gradient, the usual convective saturation[9-11] was found, but with increased growth length before spatial saturation.

Nicholson and Kaufman[1] have considered the case $V_1V_2 < 0$, and thus the possibility of absolute growth, with $\kappa(x)$ again

a turbulent function and no damping. The ratio L_T/L_0 was arbitrary. For very small rms mismatch the usual convective saturation[10,11] was found. However, for rms mismatch greater than an L_T-dependent threshold, the convective saturation disappeared, absolute growth occurring instead. For $L_T \cong L_0$, this threshold was so small that the spatial derivative of the total wavenumber mismatch, representing linear density gradient plus turbulent part, vanished nowhere in the system. An analytic approach to this problem has been given by Spatschek, Shukla, and Yu.[3]

In this paper, we take a mismatch of the form $\kappa(x) = \kappa' x + \kappa_m \sin(x/L_m)$, representing a density gradient plus a sinusoidal modulation of density. In Sec. II, we allow for only the modulation ($\kappa' = 0$), obtaining an analytic solution for the spatial growth rate, when $V_1V_2 > 0$; and for the temporal growth rate, when $V_1V_2 < 0$. In Sec. III, we include the gradient ($\kappa' \neq 0$), with $V_1V_2 < 0$, and by numerical integration of equations (1) we find that for κ_m greater than an L_m-dependent threshold, absolute growth replaces convective saturation. This result is in qualitative agreement with the result discussed above;[1] namely, that turbulent modulation in the presence of a linear density gradient can destabilize the convective saturation. In Sec. IV, we apply our results to Raman backscattering in a laser fusion geometry. Section V presents our conclusions.

II. PLASMA WITH SINUSOIDAL DENSITY MODULATION

In this section, we consider analytically an otherwise homogeneous plasma with sinusoidal density modulation, obtaining spatial growth rates for $V_1V_2 > 0$, and temporal growth rates for $V_1V_2 < 0$.

A sinusoidal density modulation is <u>like</u> turbulence in having amplitude and scale length, while it is <u>unlike</u> turbulence in not being random. Thus we expect important similarities as well as important differences in the results obtained here, as compared to turbulent results.

Eliminating a_2 from Eqs. (1) and looking for normal modes $a_1(x,t) = a_1(x)\exp(-i\omega t)$, we have

$$\left\{\partial_x^2 + \left[\frac{-i\omega + \nu_1}{V_1} + \frac{-i\omega + \nu_2}{V_2} - i\kappa(x)\right]\partial_x + \left[\frac{-i\omega + \nu_1}{V_1}\left(\frac{-i\omega + \nu_2}{V_2} - i\kappa(x)\right) - \frac{\gamma_0^2}{V_1 V_2}\right]\right\} a_1(x) = 0 \quad . \quad (2)$$

With $\kappa(x) = \kappa_m \sin(x/L_m)$, this equation is of the form

$$\left[\partial_x^2 + (A_1 + A_2 \sin x/L_m)\partial_x + (A_3 + A_4 \sin x/L_m)\right] a_1(x) = 0 \quad (3)$$

where

$$iA_1 = \frac{\omega + i\nu_1}{V_1} + \frac{\omega + i\nu_2}{V_2}$$

$$A_2 = -i\kappa_m \quad (4)$$

$$A_3 = -\frac{\gamma_0^2 + (\omega + i\nu_1)(\omega + i\nu_2)}{V_1 V_2} \quad (4)$$

$$A_4 = -\kappa_m(\omega + i\nu_1)/V_1 \quad .$$

When $\omega = \nu_1 = \nu_2 = 0$, Eq. (3) is equivalent to the well-known Ince's equation;[12,13] a simple transformation could then remove the middle

term, producing a Hill equation[12,13] of the form $\partial_x^2 a_1(x) + \left[c_1 + c_2 \cos(x/L_m) + c_3 \cos(2x/L_m)\right] a_1(x) = 0$. Only the $\cos(2x/L_m)$ term makes this equation different than the Matheiu equation. For our purposes, the present form Eq. (3) is more convenient.

The coefficients of Eq. (3) are periodic in x (with period $2\pi L_m$). Floquet's theorem then states that there exists a solution of the form $a_1(x) = \exp(ikx)\phi(x)$ with $\phi(x)$ periodic in x (with period $2\pi L_m$) and k complex in general. Such a solution can be very instructive, as we shall see below. Expressing this function $\phi(x)$ as a Fourier series $\sum_{-\infty}^{\infty} c_n \exp(inx/L_m)$, we obtain the recursion relation

$$\gamma_n^- c_{n-1} + c_n - \gamma_n^+ c_{n+1} = 0 \qquad (-\infty < n < \infty) \quad (5)$$

for the set of Fourier coefficients $\{c_n\}$, where

$$\gamma_n^{\pm} \equiv \frac{(A_2 L_m/2)(kL_m + n \pm 1) - iL_m^2 A_4/2}{L_m^2 A_3 + iL_m A_1(kL_m + n) - (kL_m + n)^2} \quad . \quad (6)$$

The set of Eqs. (5) is solved as follows. Defining

$$u_n \equiv \frac{c_{n-1}}{c_n} \quad ; \qquad v_n \equiv \frac{c_{n+1}}{c_n} \quad (7)$$

Eqs. (5) become on dividing by c_n

$$\gamma_n^- u_n + 1 - \gamma_n^+ v_n = 0 \qquad (-\infty < n < \infty) \quad . \quad (8)$$

Dividing by c_{n-1}, Eqs. (5) become

$$\gamma_n^- + v_{n-1} - \gamma_n^+(v_n/u_n) = 0 \quad . \tag{9}$$

Solving (8) for u_n and inserting u_n in (9), we find

$$\gamma_n^- + v_{n-1} + v_n\left(\frac{\gamma_n^-}{1 - \gamma_n^+ v_n}\right) = 0 \quad . \tag{10}$$

Solve (10) for v_{n-1} and shift the index up by one; then

$$v_n = -\frac{\gamma_{n+1}^-}{1 - \gamma_{n+1}^+ v_{n+1}} \tag{11}$$

which is, in continued fraction form,

$$v_n = -\frac{\gamma_{n+1}^-}{1+}\frac{\gamma_{n+1}^+\gamma_{n+2}^-}{1+}\frac{\gamma_{n+2}^+\gamma_{n+3}^-}{1+}\cdots \tag{12}$$

where each plus sign in the denominator acts on everything to the right of it. In similar fashion, we divide (5) by c_{n+1} instead of c_{n-1} to obtain

$$u_n = \frac{\gamma_{n-1}^+}{1+}\frac{\gamma_{n-1}^-\gamma_{n-2}^+}{1+}\frac{\gamma_{n-2}^-\gamma_{n-3}^+}{1+}\cdots \quad . \tag{13}$$

The solution $a_1(x) = \exp(ikx)\phi(x)$ is now completely determined. The value of k is obtained by choosing a value for n, $n = 0$ let us say, in Eq. (8), which becomes the dispersion relation

$$\left\{\frac{\gamma_0^-\gamma_{-1}^+}{1+}\frac{\gamma_{-1}^-\gamma_{-2}^+}{1+}\frac{\gamma_{-2}^-\gamma_{-3}^+}{1+}\cdots\right\} + 1 + \left\{\frac{\gamma_0^+\gamma_1^-}{1+}\frac{\gamma_1^+\gamma_2^-}{1+}\frac{\gamma_2^+\gamma_3^-}{1+}\cdots\right\} = 0 \tag{14}$$

for k as a function of ω, κ_m, and L_m. The c_n are obtained by choosing a value for c_0, and noting that from the definition (7), we

have $c_n = v_0 v_1 \cdots v_{n-2} v_{n-1} c_0$ for $n > 0$ and $c_n = u_0 u_{-1} \cdots u_{-n+2} u_{-n+1} c_0$ for $n < 0$. Thus we have constructed the complete solution aside from an arbitrary constant c_0. In this report we shall not evaluate $\{c_n\}$, but rather obtain as much information as possible from the parameter k.

A. Spatial Growth Rate for Parallel Group Velocities

With parallel group velocities, $V_1 V_2 > 0$, there is no possibility of absolute instability, and we consider the spatial response to a constant source $a_1(x = 0) = 1$, steady state in time.[15] We do this by setting the temporal growth rate $\omega = 0$ in the definition above Eq. (2), and consider Eq.(14) as a dispersion relation for the spatial growth rate k. For zero modulation, $\kappa_m = 0$, we know that the response is $\propto \exp(x/L_0)$; for finite modulation, $\kappa_m \neq 0$, we expect the spatial growth rate to be reduced. From Eqs. (4) we have for $\omega = \nu_1 = \nu_2 = 0$

$$\begin{aligned} A_1 &= 0 \\ A_2 &= -i\kappa_m \\ A_3 &= -L_0^{-2} \\ A_4 &= 0 \quad . \end{aligned} \tag{15}$$

Then from Eqs. (6)

$$\gamma_n^{\pm} = (i\kappa_m L_m/2)\frac{(kL_m + n \pm 1)}{(L_m/L_0)^2 + (kL_m + n)^2} \quad . \tag{16}$$

For small $L_m\kappa_m$, keeping only lowest order terms, the dispersion relation (14) is

$$\gamma_0^-\gamma_{-1}^+ + \gamma_0^+\gamma_1^- + 1 = 0 \qquad (17)$$

which for vanishing κ_m is only satisfied if one of the denominators in (16) vanishes, yielding the usual homogeneous spatial growth rate

$$ik = L_0^{-1} \quad . \qquad (18)$$

For small $L_m\kappa_m$, we expand Eq. (17) about $ik = L_0^{-1}$, obtaining

$$ik = L_0^{-1}\left[1 - \frac{(\kappa_m L_m)^2}{4(1 + 4L_m^2/L_0^2)}\right] \quad . \qquad (19)$$

We see from (19) that for fixed κ_m the decrease in growth rate is most pronounced for large modulation wavelength $L_m \gtrsim L_0$.

For arbitrary $L_m\kappa_m$, we solve (14) numerically, keeping as many terms as necessary in the continued fractions. The results are shown in Fig. 1 for $L_m/L_0 = 1$, and in Fig. 2 for $L_m/L_0 = 0.5$. The spatial growth rate decreases with increasing modulation κ_m until a certain point, where it reaches zero and bounces up again. For completeness, we have shown the positive and negative roots, both of which are purely real.

B. Temporal Growth Rate for Antiparallel Group Velocities

If $V_1V_2 < 0$, it is no longer appropriate to consider a steady state in time, so we consider a different, physically relevant problem. We ask the question: What is the temporal response of the system to the uniform initial conditions $a_1(x,t = 0) =$ constant, $a_2(x,t = 0) = 0$? We expect to find a temporal growth rate $\mathrm{Im}(\omega)$

which in the limit $\kappa_m \to 0$ reduces to the usual homogeneous result $\mathrm{Im}(\omega) = \gamma_0$. The basic equation (3) is periodic, and the initial conditions are periodic; we may thus look for a periodic solution, which means setting $k = 0$. Then Eq. (14) becomes a dispersion relation for ω.

In this case, taking $\nu_1 = \nu_2 = 0$, $V_1 > 0$, $V_2 < 0$, we have from (4)

$$\begin{aligned} A_1 &= -i\omega\left(\frac{1}{V_1} + \frac{1}{V_2}\right) \\ A_2 &= -i\kappa_m \\ A_3 &= -L_0^{-2}(\omega^2/\gamma_0^2 + 1) \\ A_4 &= -\omega\kappa_m/V_1 \quad . \end{aligned} \qquad (20)$$

Then (6) becomes

$$\gamma_n^{\pm} = \frac{(-i\kappa_m L_m/2)\left[n \pm 1 - \left(\frac{L_m}{L_0}\right)\left(\frac{\omega}{\gamma_0}\right)\left(\frac{-V_2}{V_1}\right)^{\frac{1}{2}}\right]}{(L_m/L_0)^2(\omega^2/\gamma_0^2 + 1) + n(L_m/L_0)(\omega/\gamma_0)\left(\sqrt{\frac{-V_2}{V_1}} - \sqrt{\frac{-V_1}{V_2}}\right) - n^2} \qquad (21)$$

For $\kappa_m L_m$ small, we can again use the simplifed dispersion relation (17), which in the limit $\kappa_m L_m \to 0$ yields $\omega = i\gamma_0$ as expected. For small but finite $\kappa_m L_m$, Eq. (17) predicts, for the special case $V_2 = -V_1$,

$$\omega = i\gamma_0\left(1 - \frac{\kappa_m^2 L_m^2}{4}\right) \quad ; \quad \kappa_m L_m \ll 1 \quad . \qquad (22)$$

The decrease in temporal growth rate is proportional to the square of the modulation, and is most pronounced for large modulation wavelength.

In addition to the root discussed in the previous paragraph, there are an infinite number of other roots of the full dispersion relation (14). For $\kappa_m L_m \to 0$, $V_2 = -V_1$, the roots occur at

$$\frac{\omega}{\gamma_0} = \pm i(1 - n^2 L_0^2/L_m^2)^{\frac{1}{2}} \qquad 0 \le n < \infty \quad . \qquad (23)$$

This infinite set of roots is reminiscent of the theory of wave propagation in periodic media, where there are an infinite number of roots $\omega(k = 0)$, one root per Brillouin zone.[16] We are also reminded of the infinite set of eigenfrequencies found in the theory of parametric instabilities in finite media.[15,17-21]

For finite κ_m, we expect one branch of the graph ω vs κ_m associated with each root (23). In Fig. 3 are shown the roots ω vs κ_m for $L_m/L_0 = 0.25$, $V_2 = -V_1$, $\nu_1 = \nu_2 = 0$. For these parameters, if ω is a root of (14), so is $-\omega$ and so is $-\omega^*$. From Eq. (23), we have $\omega(\kappa_m \to 0) = \pm i, \pm\sqrt{15}, \cdots$. Over the range of κ_m shown, $\mathrm{Re}(\omega)$ is almost constant for each branch; we display only $\mathrm{Im}(\omega)$ in Fig. 3. For increasing κ_m, the unstable root (at $\kappa_m \to 0$) decreases, reaching zero eventually. Before it reaches zero, however, the imaginary part of the stable root (at $\kappa_m \to 0$) overtakes it and becomes the most unstable root. It appears that this behavior will continue indefinitely, roots of higher n obtaining substantial imaginary parts with increasing κ_m; furthermore, the roots of lower n show a bouncing behavior as a function of κ_m. Thus, the envelope of

most unstable $\mathrm{Im}(\omega)$ appears as in Fig. 4, for $L_m/L_0 = 1$, $V_2 = -V_1$, $\nu_1 = \nu_2 = 0$. The envelope $\mathrm{Im}(\omega)$ never becomes exactly zero for finite κ_m, rather asymptoting to zero for $\kappa_m \to \infty$. For modulation amplitude $L_0\kappa_m$ slightly above zero, the growth rate $\mathrm{Im}(\omega)$ falls off much more rapidly for $L_m/L_0 = 1$ (Fig. 4) than for $L_m/L_0 = 0.25$ (Fig. 3), as predicted by Eq. (22). However, the envelope of $\mathrm{Im}(\omega)$ for large $L_0\kappa_m \approx 10$ about the same magnitude in both cases.

For $\kappa_m \to 0$, the growth rate $\mathrm{Im}(\omega) = \gamma_0$ calculated here is also the growth rate of the peak of the pulse response to the initial conditions $a_1(x,t = 0) = \delta(x)$, $a_2(x,t = 0) = 0$, i.e., the Green's function problem.[22] We ask the question: For $\kappa_m > 0$, does the fastest growing root of the dispersion relation (14) still correspond to the growth rate of the Green's function pulse, as measured by an observer moving with the pulse? The answer is yes. In Fig. 3, the points are the pulse growth rates as obtained by direct numerical integration of Eqs. (1) for finite κ_m. We see that they agree with the fastest growing root of the dispersion relation (14), within the accuracy of the numerical integration. Note that this agreement can not be predicted by Bers-Briggs analysis,[23] since we are dealing with an inherently inhomogeneous system.

What have we learned from this model of a homogeneous plasma with a superimposed density modulation? We have learned that the modulation tends to reduce growth rates, both spatial and temporal. The reduction is greatest for large modulation wavelengths; inhomogeneities of size $\gtrsim L_0$ have the greatest effect on the coupled mode equations (1). We may expect that these results apply also to the

case of turbulent inhomogeneities. Furthermore, the regular nature of the sinusoidal modulation leads to features in the behavior of growth rate as a function of modulation amplitude, such as the bouncing phenomena in Figs. 1-4, which we would not necessarily expect to find in the case of turbulent inhomogeneities.

In the next section, we consider the simple model of a sinusoidal modulation superimposed on a linear density ramp. Once again, important similarities to the turbulent case are found.

III. LINEAR DENSITY GRADIENT WITH SINUSOIDAL DENSITY MODULATION

We consider next a sinusoidal density modulation in the presence of a linear density gradient. We restrict ourselves to anti-parallel group velocities, and take the wave number mismatch to be

$$\kappa(x) = \kappa' x + \kappa_m \sin(x/L_m) \quad . \tag{24}$$

For small κ_m, we expect to recover the usual convective saturation. For larger κ_m, we might expect to destabilize the convective saturation, just as turbulence did in Ref. 1.

We numerically integrate the basic equations (1), with the form (24) for $\kappa(x)$ and with Green's function initial conditions. We indeed find convective saturation for small κ_m, and we indeed find absolute instability for κ_m greater than an L_m-dependent threshold. In Fig. 5 we show the absolute growth rate, obtained with $V_2 = -V_1$, $L_0^2\kappa' = 1$, $\nu_1 = \nu_2 = 0$, $L_m/L_0 = 0.8$. Above threshold, the growth rate rises rapidly to nearly the homogeneous medium growth rate.

In the example shown in Fig. 5, the threshold value of κ_m occurs at $L_0\kappa_m \approx 0.1$. As in the turbulent case of Ref. 1, this value of $L_0\kappa_m$ is far below that required for the vanishing of the derivative of the wave number mismatch $\kappa(x)$; i.e., $d\kappa(x)/dx = \kappa' + (\kappa_m/L_m)\cos(x/L_m) = 0$ implies (with $L_0^2\kappa' = 1$ and $L_m/L_0 = 0.8$) that $L_0\kappa_m = 0.8$, a much higher value of $L_0\kappa_m$ than the observed threshold $L_0\kappa_m \approx 0.1$.

We next consider a shorter wavelength modulation, $L_m/L_0 = 0.18$, in Fig. 6. Here we see a much less violent instability, the maximum growth rate being only $\mathrm{Im}(\omega)/\gamma_0 \approx 0.2$. Furthermore, the threshold value of κ_m is $L_0\kappa_m \approx 1.0$, much higher than would be predicted by setting $d\kappa(x)/dx = 0$, yielding here $L_0\kappa_m = 0.18$.

Our conclusion from the last two paragraphs is that the modulation wavelength is the relevant parameter in determining the tendency of the system toward absolute instability, rather than considerations of the vanishing of the derivative of the wave number mismatch $\kappa(x)$. This conclusion is emphasized in Fig. 7, where we hold the modulation amplitude fixed at a value $L_0\kappa_m = 2$ ($V_2 = -V_1$, $L_0^2\kappa' = 1$) and vary the modulation wavelength. We find that the absolute growth rate is substantial for $L_m \sim L_0$, falling off rapidly for $L_m \ll L_0$ and for $L_m \gg L_0$.

In Fig. 8, we display the results of Figs. 5, 6, and 7 as a three dimensional plot of absolute growth rate γ vs κ_m and L_m. The dashed curve is schematic, showing the inferrred threshold for absolute instability in the κ_m-L_m plane. For large κ_m, the threshold value of L_m approaches zero. For both large and small L_m, the

threshold value of κ_m is large, demonstrating once again that the most effective inhomogeneities are those with scale length $\sim L_0$.

We interpret these results in terms of the concept of mathematical reflections. When the inhomogeneities are of a size near the all important length L_0, constructive interferences between solutions of our second order system Eqs. (1) lead to instability. When the inhomogeneities are of a size much smaller or greater than L_0, the system feels only the monotonic part of $\kappa(x)$, given by $\kappa' x$, and exhibits the usual convective saturation. This saturation we interpret as a destructive interference between solutions of our second order set Eqs. (1).

The detailed space-time response of the system, to the initial conditions $a_1(x,t=0) = \delta(x)$, $a_2(x,t=0) = 0$, is of interest in its own right. For the parameters of Fig. 7 ($L_0\kappa_m = 2$, $V_2 = -V_1$, $L_0^2\kappa' = 1$) we choose a value for the modulation wavelength, $L_m/L_0 = 0.16$, which is just barely above the threshold for absolute instability. Figure 9 shows the space-time behavior of $a_2(x,t)$ at four different times, $\gamma_0 t = 7,13,16,20$. At $\gamma_0 t = 7$, the usual convective saturation has set in. At the substantially later time $\gamma_0 t = 13$, the saturated behavior persists, but with many more fluctuations. The hint of things to come is shown by the enhanced fluctuation at $x = 0$, in the middle of the figure. At $t = 16$, this enhanced fluctuation has grown rapidly to tower over the rest of the pulse shape. After a period of rapid growth, the enhanced fluctuation at $x = 0$ itself saturates. This saturated state, shown at $\gamma_0 t = 20$, has its own enhanced fluctuations at the very center which foretell the outburst of yet a third period of rapid growth, and so on ad infinitum.

To conclude, we have seen that the behavior of the system of Eqs. (1) with the wavenumber mismatch $\kappa(x) = \kappa' x + \kappa_m \sin(x/L_m)$ is qualitatively similar to the turbulent case of Ref. 1. Absolute instability results for wavelengths $L_m \sim L_0$, and for modulation amplitudes one order of magnitude smaller than that required to make $d\kappa(x)/dx = 0$. The instability growth rate is very sensitive to modulation wavelength L_m, falling off rapidly for $L_m \lesssim L_0$.

IV. RAMAN BACKSCATTERING EXAMPLE

Let us apply our results to the physical example of Raman backscattering,[24,25] where an electromagnetic wave decays into another electromagnetic wave plus a Langmuir wave, in laser fusion geometry. Consider a homogeneous plasma of electron temperature $T_e \tilde{=} 1$ KeV, and plasma frequency $\omega_p = \omega_0/3$, where $\omega_0 = 2 \times 10^{15} s^{-1}$ is the frequency of a Nd:glass laser of intensity $I_0 = 10^{15}$ W/cm^2. Working to 10% accuracy, the group velocities of the two waves are $V_1 \tilde{=} c$ and $V_2 = 3 v_e^2 k_2/\omega_2 \tilde{=} -0.3\, c$. The pump parameter is $\gamma_0 = (v_0/c)(\omega_0\omega_p)^{\frac{1}{2}} \tilde{=} 4 \times 10^{13} s^{-1}$, where v_0 is the maximum oscillation velocity of an electron in the field of the laser. Thus we find $L_0 = (|V_1 V_2|)^{\frac{1}{2}}/\gamma_0 = 1.3$ μm. This value of L_0 is only somewhat greater than the free space wavelength $\lambda_0 = 1.06$ μm, which means that we are pushing to the limits of validity of Eqs. (1); their derivation requires all spatial quantities to be much larger than the three basic wavelengths.

The wave number mismatch is related to density perturbations through the dispersion relations of the three basic modes; to 10% accuracy we need only consider the electrostatic mode. The dimensionless wave number mismatch $L_0\kappa_m$ is then related to the relative plasma density fluctuation Δ_n by

$$L_0\kappa_m = \frac{(k_2L_0)}{6(k_2\lambda_D)^2}\Delta_n = 36\,\Delta_n \qquad (25)$$

where k_2 is the electrostatic wavenumber and λ_D is the Debye length.

The temporal growth rate for small κ_m, obtained by generalizing Eq. (22) to arbitrary V_2/V_1, is in physical units

$$\frac{\mathrm{Im}(\omega)}{\gamma_0} = 1 - \frac{(L_m\kappa_m/2)^2}{1 + (L_m/L_0)^2\left(\left|\frac{V_1}{V_2}\right|^{\frac{1}{2}} - \left|\frac{V_2}{V_1}\right|^{\frac{1}{2}}\right)^2}\ ; \quad L_m\kappa_m \ll 1\ . \qquad (26)$$

In the present example $|V_2/V_1| = 0.03$; then for $L_m \gtrsim L_0$ we can neglect the first term in the denominator, and using (25) we obtain

$$\frac{\mathrm{Im}(\omega)}{\gamma_0} = 1 - \frac{(L_0\kappa_m)^2}{120} = 1 - 11\,\Delta_n^2\ . \qquad (27)$$

Equation (27) predicts roughly a 10% decrease in Raman instability growth rate for a 10% density fluctuation. This insensitivity of growth rate to relative density fluctuation tends to support the conjecture of Kaw et al.,[2] that very short wavelength turbulence, which can not be studied in the context of our WKBJ equations (1), will be more effective in suppressing Raman instability than the long wavelength turbulence studied here.

While we have not considered the example of this section in the presence of a linear density gradient, we have performed the related calculation[26] with a turbulent wave number mismatch, of correlation length $L_T/L_0 = 1.3$, in the presence of a linear density gradient of scale length 100 μm. It is found that a relative density

fluctuation $\Delta_n \cong 10^{-3}$ is sufficient to destabilize the convective saturation; the absolute growth rate rises rapidly with increasing relative density fluctuation, to greater than one half its uniform medium value.

V. CONCLUSIONS

Sinusoidal density modulation of an otherwise homogeneous plasma tends to reduce spatial and temporal parametric instability growth rates. For the Raman backscatter example considered, substantial growth rate reduction requires fairly large density modulation.

In the presence of a linear density gradient, small amounts of sinusoidal density modulation can destabilize the convective saturation, allowing absolute growth. The qualitative agreement of this result with previous results[1] for a turbulent density gradient lead us to conclude that the amplitude and scale length of the density perturbation, rather than the detailed spatial profile, is important.

ACKNOWLEDGMENT

I thank Allan Kaufman for suggesting this problem, and for valuable insights along the way. I thank B. Cohen, G. Johnston, S. Johnston, M. Mostrom, and G. Smith for useful discussions.

FOOTNOTES AND REFERENCES

* This work was supported by the U. S. Energy Research and Development Administration.

† Present address: Department of Astro-Geophysics, University of Colorado, Boulder, Colorado 80302.

1. Dwight R. Nicholson and Allan N. Kaufman, Phys. Rev. Lett. 33 1207 (1974).
2. P. Kaw, R. White, D. Pesme, M. Rosenbluth, G. Laval, R. Varma, and R. Huff, Comments Plasma Phys. Controlled Fuison 2, 11 (1974).
3. K. H. Spatschek, P. K. Shukla, and M. Y. Yu, Phys. Letters 51A, 183 (1975).
4. V. V. Tamoikin and S. M. Fainshtein, Sov. Phys. JETP 35, 115 (1972).
5. H. Wilhelmsson, Physica Scripta 9, 61 (1974).
6. J. J. Thomson, Finite Bandwidth Effects on the Parametric Instability in an Inhomogeneous Plasma, UCRL-79538, August, 1974 (to be published).
7. R. Pellat, D. Pesme, and G. Laval, in Proceedings of the Fifth Annual Anomalous Absorbtion Conference, Los Angeles, April, 1975.
8. M. N. Rosenbluth and E. A. Williams, in Proceedings of the Fifth Annual Anomalous Absorbtion Conference, Los Angeles, April, 1975.
9. K. J. Harker and F. W. Crawford, J. Geophys. Res. 75, 5459 (1970).
10. A. D. Piliya, Sov. Phys. JETP 37, 629 (1973).
11. M. N. Rosenbluth, Phys. Rev. Lett. 29, 565 (1972).
12. F. M. Arscott, Periodic Differential Equations (Pergamon Press, Oxford, 1964).

13. W. Magnus and S. Winkler, Hill's Equation (Interscience Publishers, New York, 1966).

14. Since we are dealing with only one solution of the second order Eq. (3), we might inquire as to the nature of the other solution. Often, there will be two linearly independent solutions of Floquet form. This is the case in Section II-A, where we have $\nu_1 = \nu_2 = \omega = 0$. In Section II-B with nonzero ω, Eq. (3) is more complicated and we remain ignorant of the second solution. Here we are only interested in finding those values of ω consistent with a solution of Floquet form with $k = 0$.

15. D. L. Bobroff and H. A. Haus, J. Appl. Phys. 38, 390 (1967).
16. C. Kittel, Introduction to Solid State Physics (Wiley, New York, 1971).
17. N. M. Kroll, J. Appl. Phys. 36, 34 (1965).
18. D. Pesme, G. Laval, and R. Pellat, Phys. Rev. Lett. 31, 203 (1973).
19. D. F. Dubois, D. W. Forslund, and E. A. Williams, Phys. Rev. Lett. 33, 1013 (1974).
20. S. S. Jha and S. Srivastava, Phys. Rev. A11, 378 (1975).
21. F. Chambers and A. Bers (M.I.T.), private communication, February 1975.
22. B. D. Fried, G. Schmidt, and R. W. Gould, Proceedings Sixth European Conference on Controlled Fusion and Plasma Physics, page 477 (1972).
23. R. Briggs, Electron Stream Interaction With Plasmas (MIT Press, Cambridge, Massachusetts, 1964).

24. J. Drake, P. Kaw, Y. C. Lee, G. Schmidt, C. S. Liu, and M. N. Rosenbluth, Phys. Fluids 17, 778 (1974).

25. C. S. Liu, M. N. Rosenbluth, and R. B. White, Phys. Fluids 17, 1211 (1974).

26. Dwight R. Nicholson, Parametric Instabilities in Inhomogeneous Plasma, Lawrence Berkeley Laboratory Report LBL-3267, June 1975 (Ph.D. Thesis).

FIGURE CAPTIONS

Fig. 1. Spatial growth rate vs modulation amplitude. ($V_2/V_1 = 1$, $\nu_1 = \nu_2 = 0$). The roots shown are purely imaginary. $\kappa(x) = \kappa_m \sin(x/L_m)$.

Fig. 2. Spatial growth rate vs modulation amplitude. ($V_2/V_1 = 1$, $\nu_1 = \nu_2 = 0$). The roots shown are purely imaginary. $\kappa(x) = \kappa_m \sin(x/L_m)$.

Fig. 3. Temporal growth rate vs modulation amplitude. ($V_2/V_1 = -1$, $\nu_1 = \nu_2 = 0$). The dots are growth rates of the pulse response to the initial conditions $a_1(x,t = 0) = \delta(x)$, $a_2(x,t = 0) = 0$, obtained by numerical integration of Eqs. (1). $\kappa(x) = \kappa_m \sin(x/L_m)$.

Fig. 4. Temporal growth rate vs modulation amplitude. ($V_2/V_1 = -1$, $\nu_1 = \nu_2 = 0$). $\kappa(x) = \kappa_m \sin(x/L_m)$.

Fig. 5. Temporal growth rate vs modulation amplitude. ($V_2/V_1 = -1$, $\nu_1 = \nu_2 = 0$, $L_0^2\kappa' = 1$). $\kappa(x) = \kappa' x + \kappa_m \sin(x/L_m)$.

Fig. 6. Temporal growth rate vs modulation amplitude. ($V_2/V_1 = -1$, $\nu_1 = \nu_2 = 0$, $L_0^2\kappa' = 1$). $\kappa(x) = \kappa' x + \kappa_m \sin(x/L_m)$.

Fig. 7. Temporal growth rate vs modulation wavelength. ($V_2/V_1 = -1$, $\nu_1 = \nu_2 = 0$, $L_0^2\kappa' = 1$). $\kappa(x) = \kappa' x + \kappa_m \sin(x/L_m)$.

Fig. 8. Temporal growth rate vs modulation amplitude and modulation wavelength. ($V_2/V_1 = -1$, $\nu_1 = \nu_2 = 0$, $L_0^2\kappa' = 1$). $\kappa(x) = \kappa' x + \kappa_m \sin(x/L_m)$. Includes data of Figs. 5, 6, and 7.

Fig. 9. Space-time response to the initial conditions $a_1(x,t = 0) = \delta(x)$, $a_2(x,t = 0) = 0$. $\kappa(x) = \kappa' x + \kappa_m \sin(x/L_m)$. ($V_2/V_1 = -1$, $\nu_1 = \nu_2 = 0$, $L_0^2\kappa' = 1$, $L_0\kappa_m = 2$, $L_m/L_0 = 0.16$).

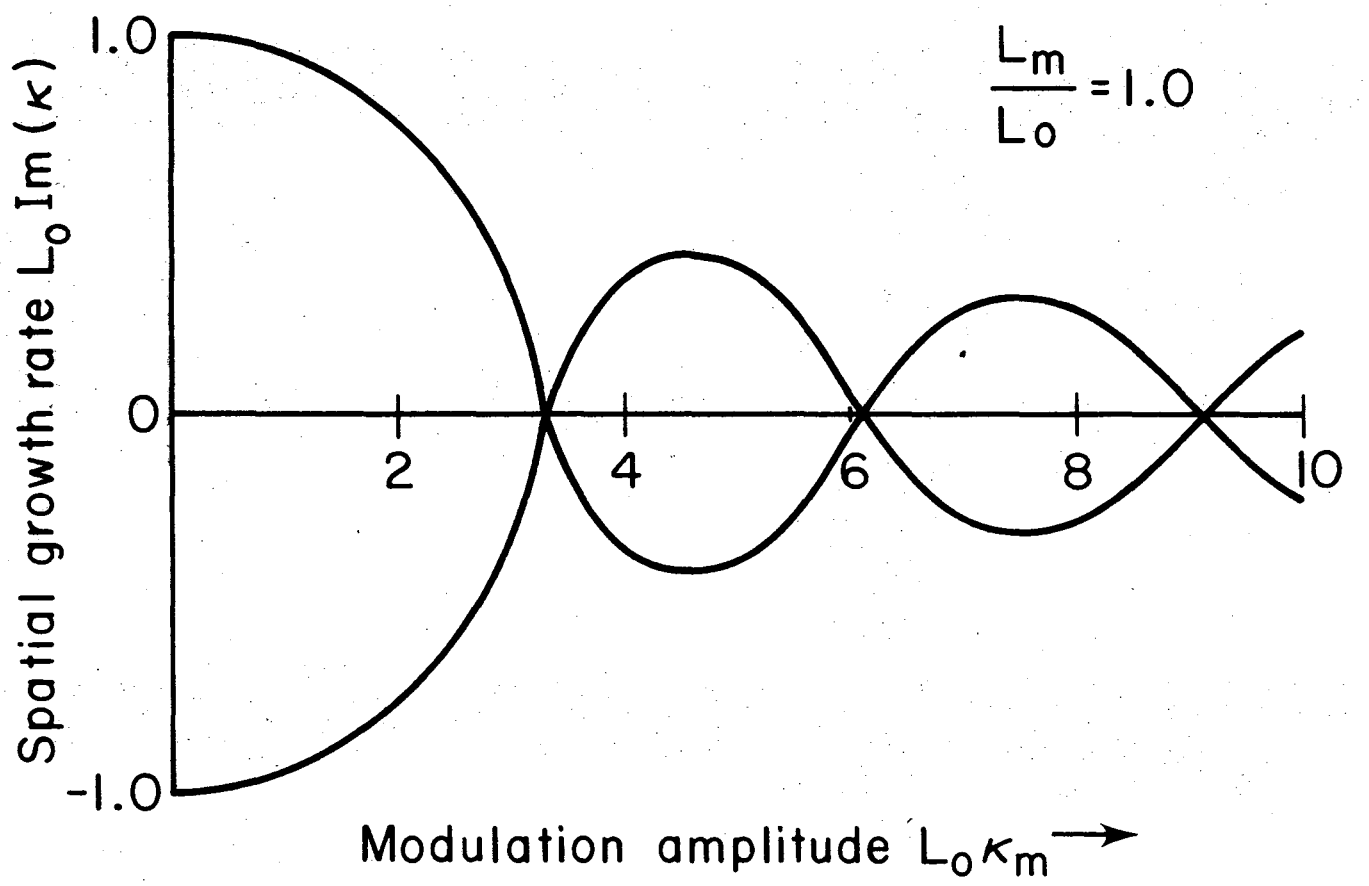

Fig. 1

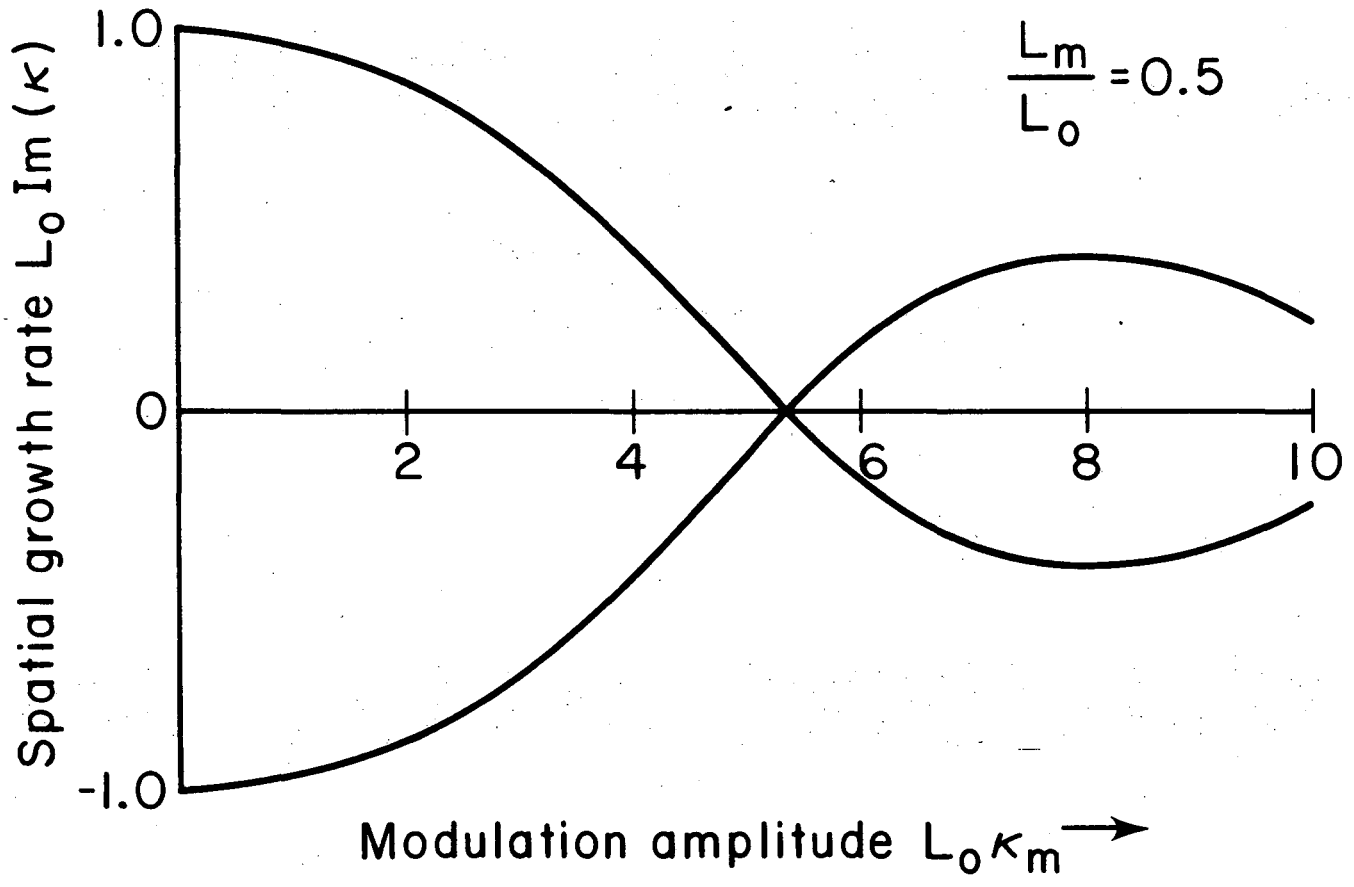
1.0
0
-1.0
Spatial growth rate L_o Im (κ)
$\frac{L_m}{L_o} = 0.5$
2
4
6
8
10
Modulation amplitude $L_o \kappa_m$
XBL757-3358A

Fig. 2

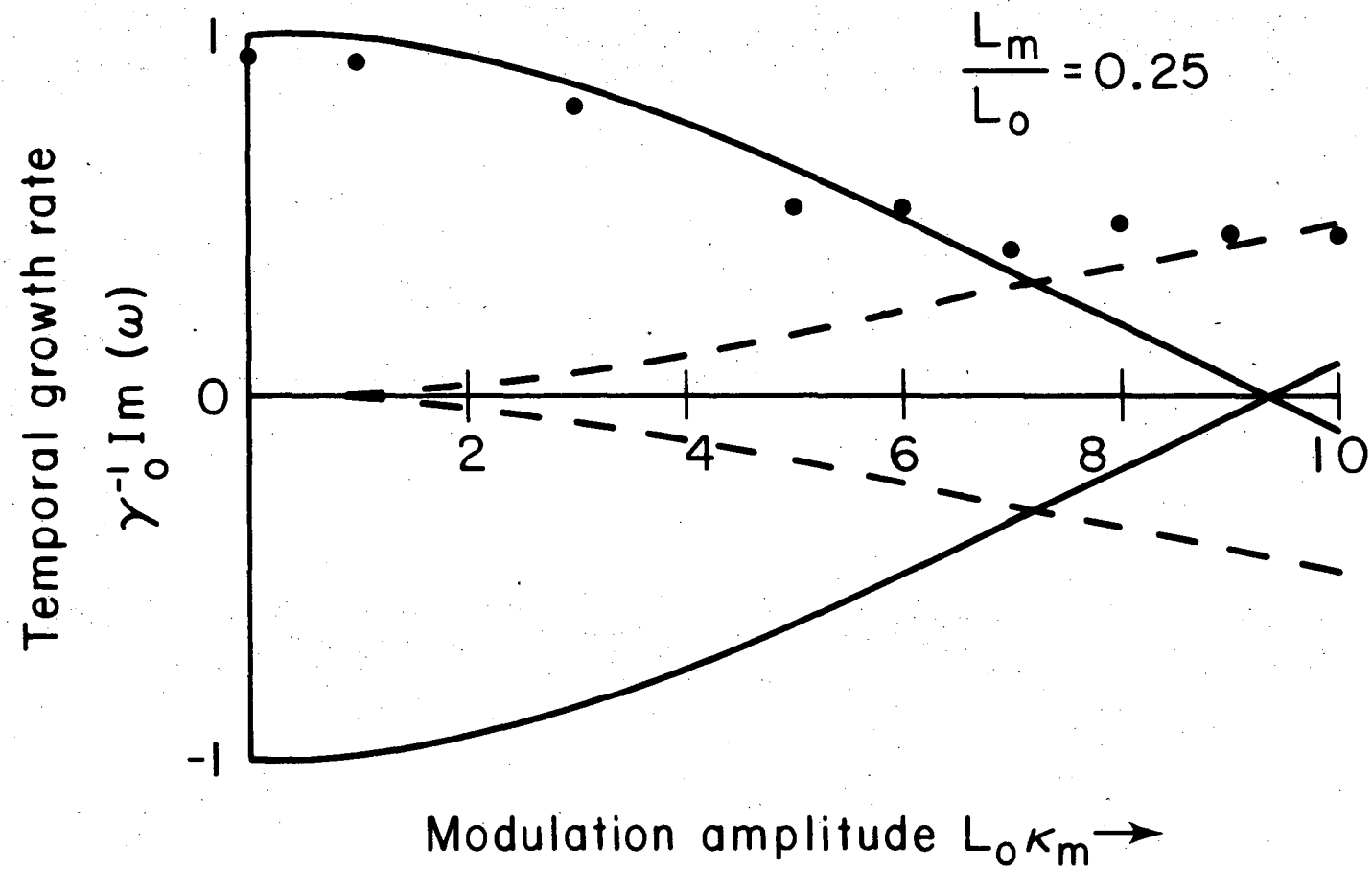

XBL758-3648A

Fig. 3

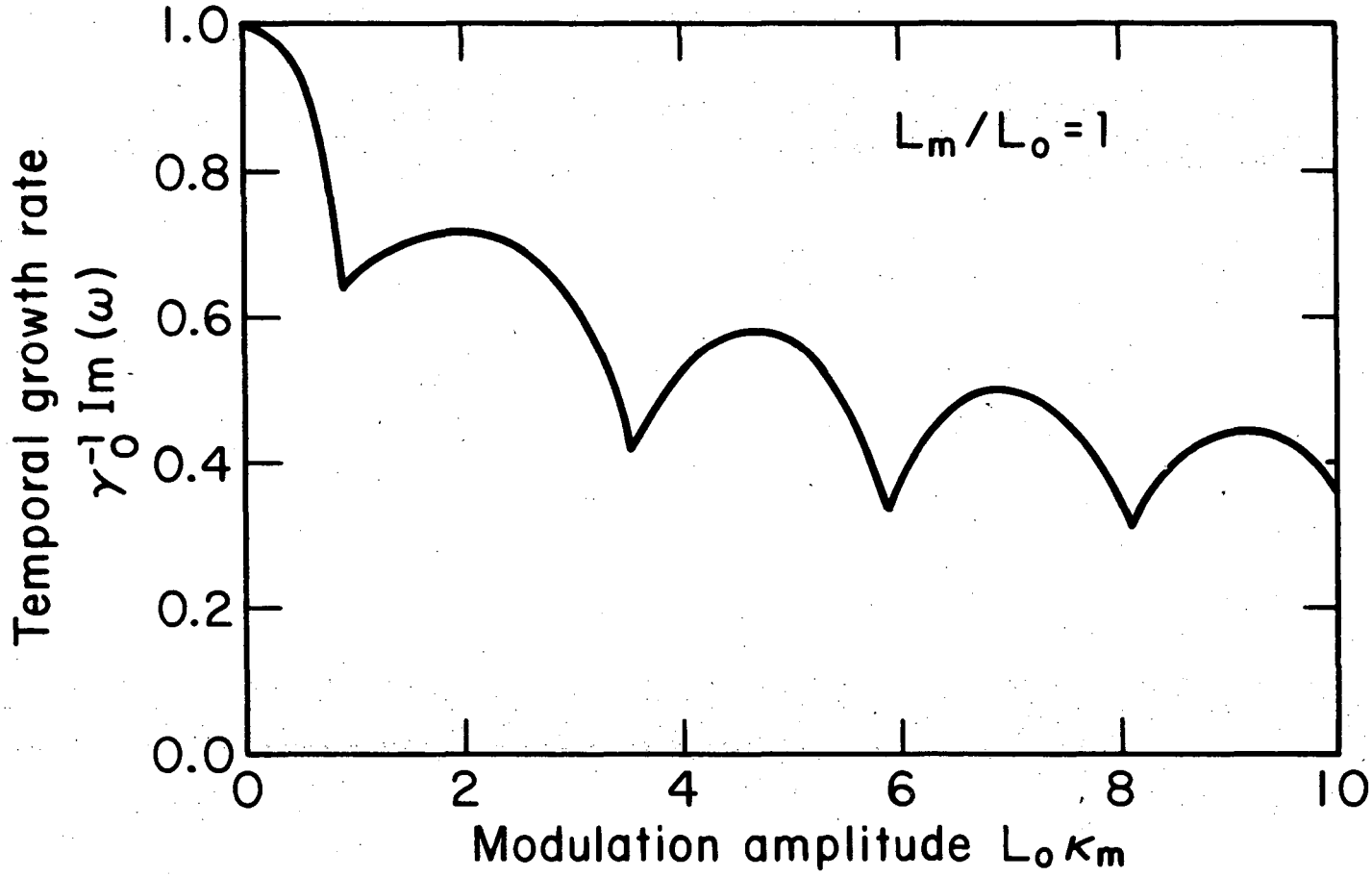

XBL757-3464

Fig. 4

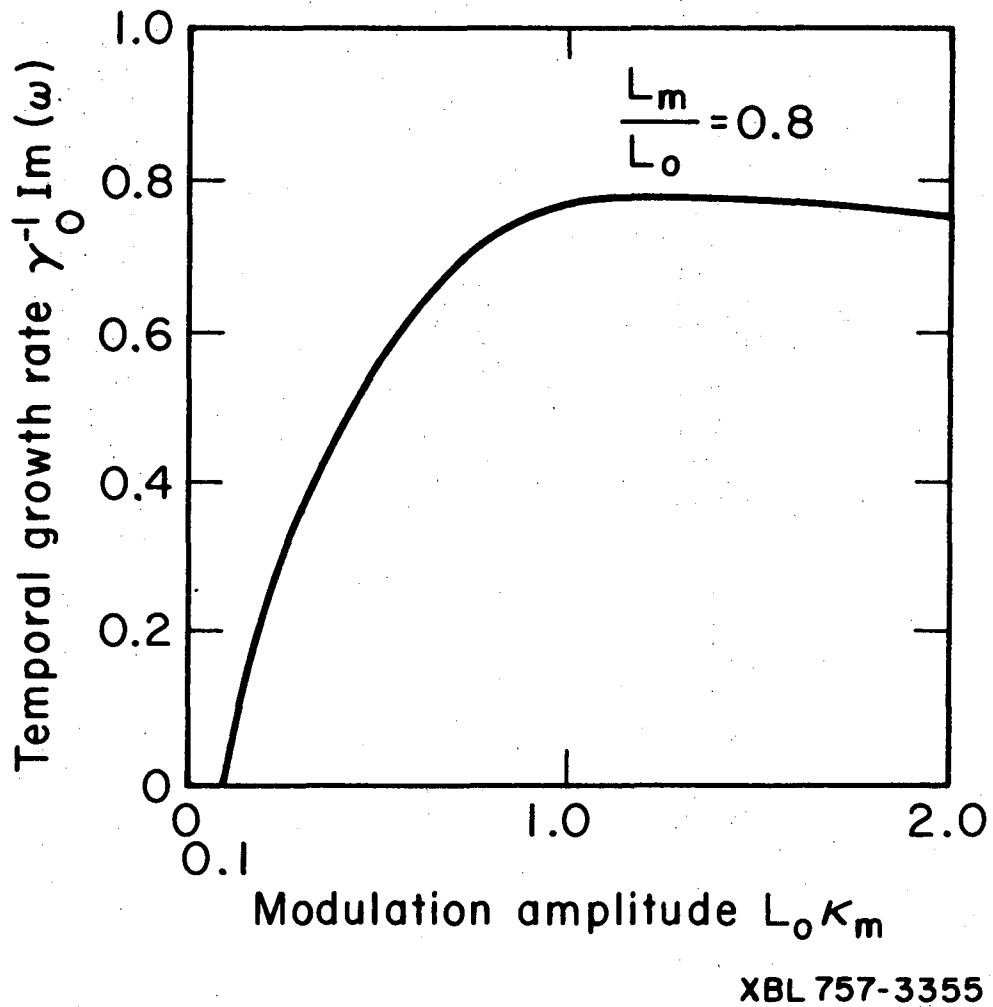

XBL 757-3355

Fig. 5

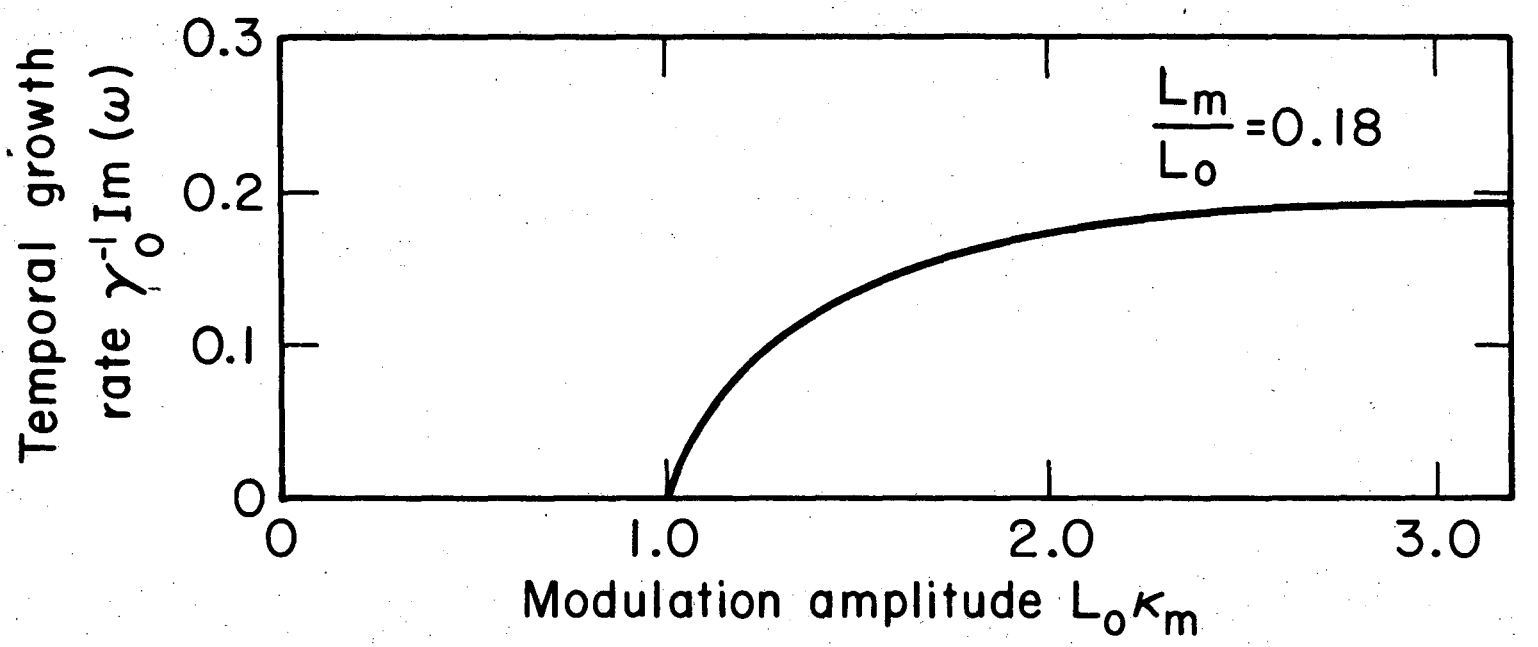
Temporal growth rate $\gamma_0^{-1} \mathrm{Im}(\omega)$
0.3
0.2
0.1
0
0
1.0
2.0
3.0
Modulation amplitude $L_0 \kappa_m$
$\frac{L_m}{L_0} = 0.18$
XBL757-3356

Fig. 6

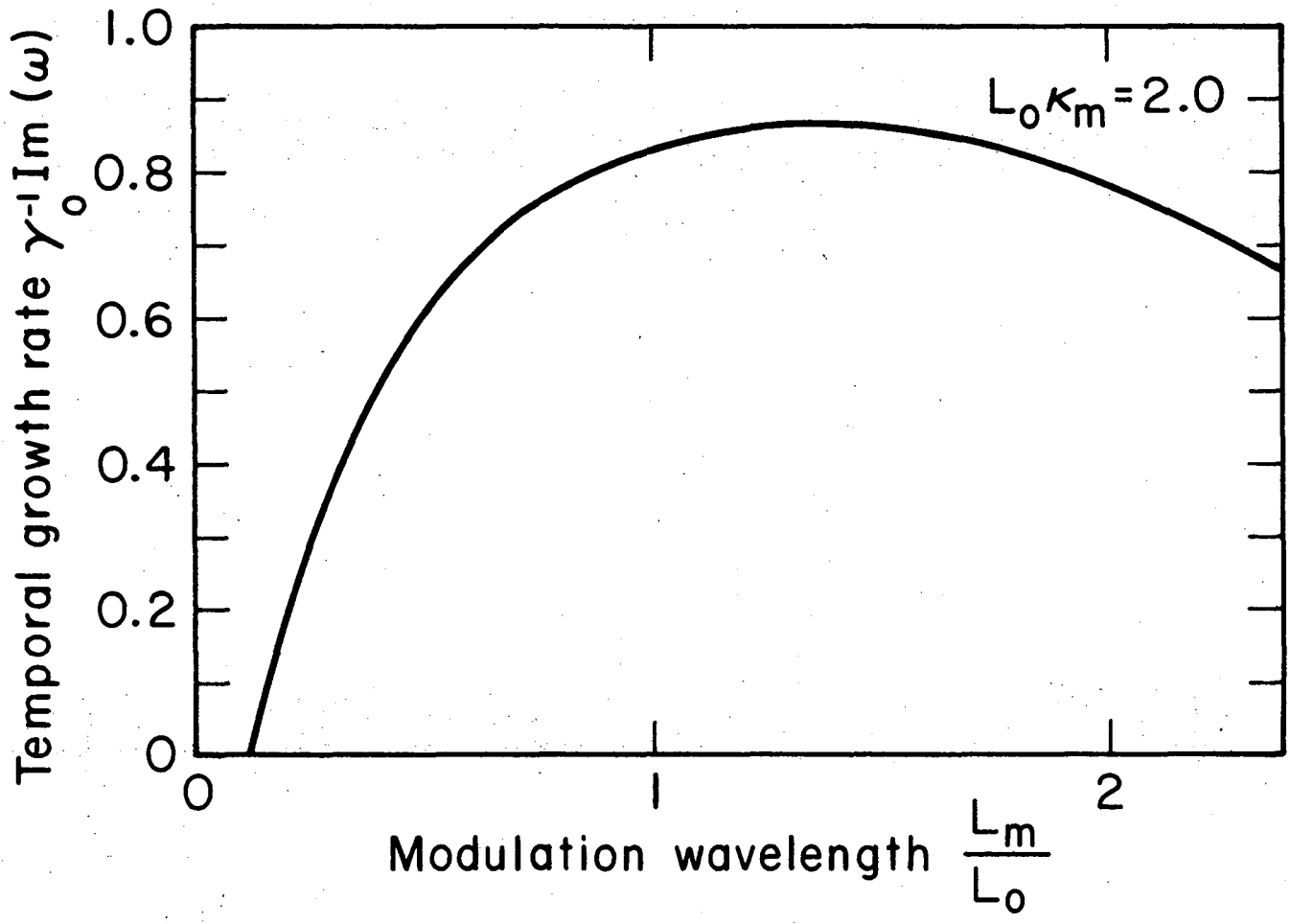

Fig. 7

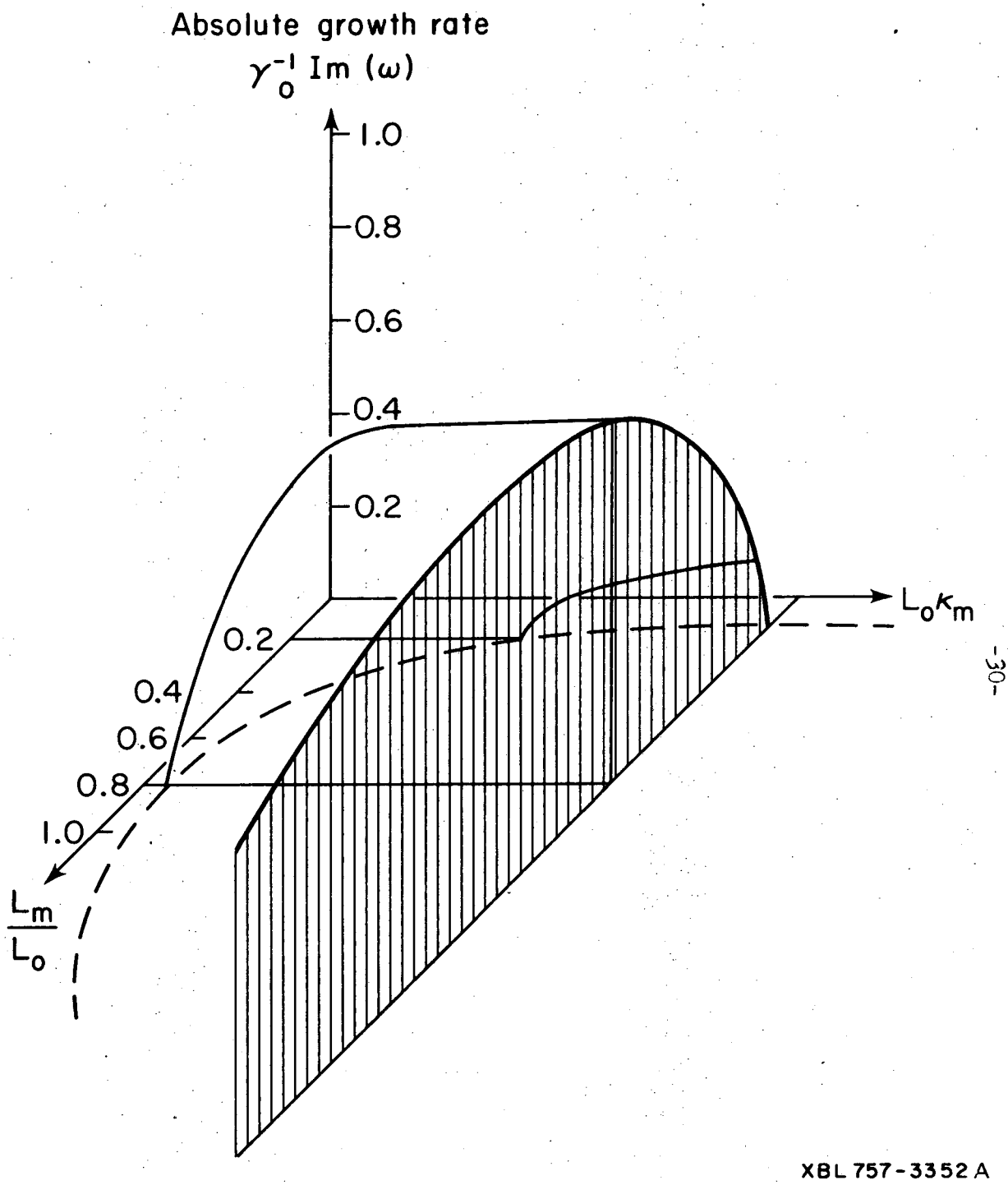

XBL 757-3352 A

Fig. 8

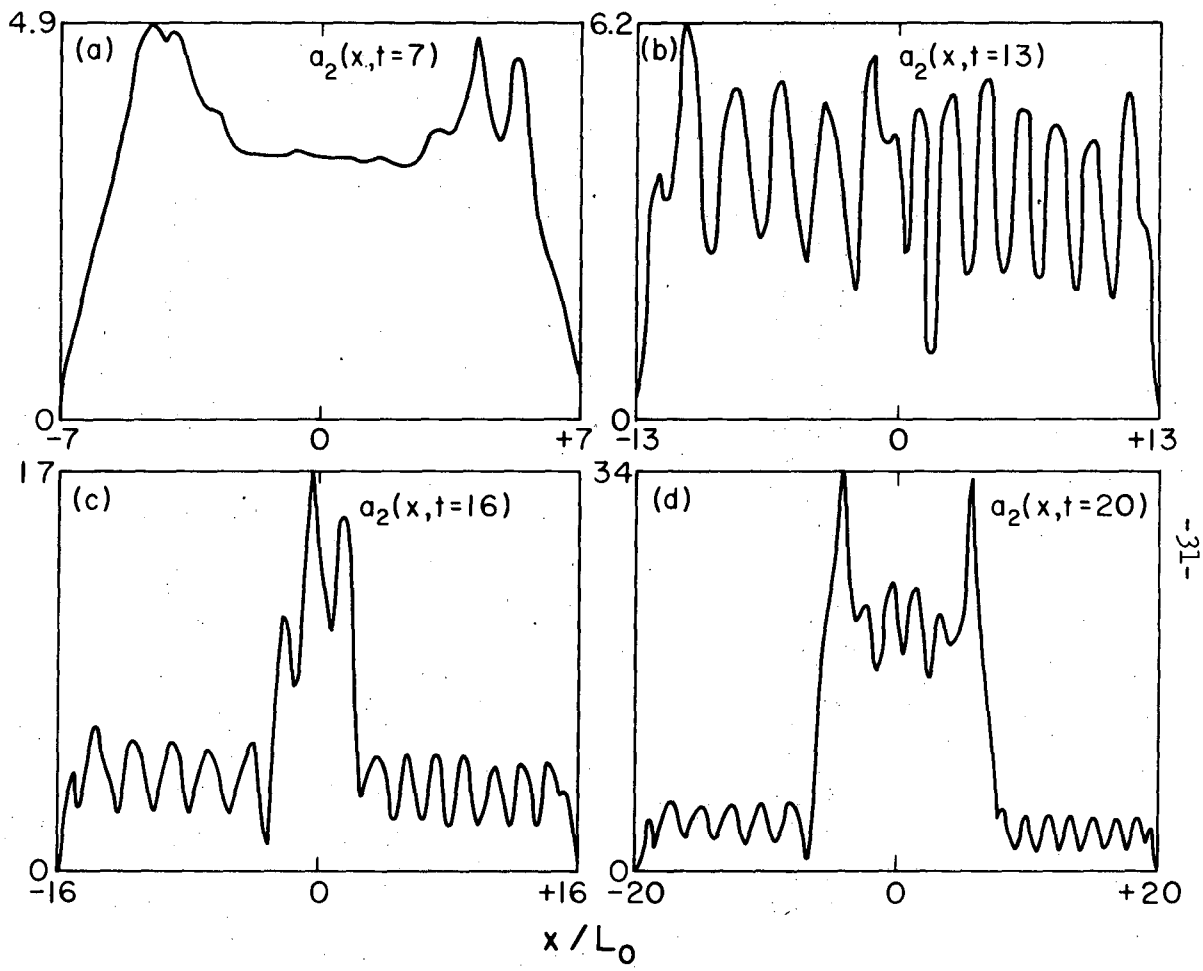

XBL 757-3361A

Fig. 9

TECHNICAL INFORMATION DIVISION
LAWRENCE BERKELEY LABORATORY
UNIVERSITY OF CALIFORNIA
BERKELEY, CALIFORNIA 94720